

# Evaluation of the ECAT EXACT HR+ 3-D PET Scanner in $H_2^{15}O$ Brain Activation Studies: Dose Fractionation Strategies for rCBF and Signal Enhancing Protocols

J. J. Moreno-Cantú, C. J. Thompson,\* and R. J. Zatorre

**Abstract**— We evaluated the performance of the ECAT EXACT HR+ 3-D whole-body positron emission tomography (PET) scanner when employed to measure brain function using  $H_2^{15}O$  bolus activation protocols that are completed in single same-day data acquisition sessions. Using vibrotactile and auditory stimuli as independent activation tasks, we studied the scanner performance under different imaging conditions in five healthy volunteers. Cerebral blood flow images were acquired from each volunteer using  $H_2^{15}O$  bolus injections of activity varying from 5–20 mCi. One-session dose-fractionation strategies were analyzed for rCBF, standard activity-concentration, switched, and cold-bolus/switched protocols. *Performance characteristics.* The scanner dead time grew linearly with injected dose from 10% to 25%. Random events varied from 30% to 50% of the detected events. Random and scattered events were corrected adequately at all doses. Estimated noise-effective-count curves plateau at about 10 mCi. *One-session 12-injection bolus PET activation protocols.* Using an acquisition protocol that accounts for the scanner performance and the practical aspects of imaging volunteers and neurological patients in a single same-day session, we assessed the correlation between the significance of activation foci and the dose/injection used. The one-session protocol employs 12 bolus injections/subject. We present evidence suggesting that when an rCBF protocol is used, image noise is reduced significantly when the activity injected increases from 5 to 10 mCi. Increasing the dose from 10 to 15 or 20 mCi yielded further but smaller reductions. Our observations also suggest that image noise will be strongly reduced if a 20-mCi dose/injection is used when data are collected using protocols that employ long acquisition times such as a switched or a cold-bolus/switched protocol.

**Index Terms**—Activation studies, ECAT HR+,  $H_2^{15}O$ , PET.

## I. INTRODUCTION

**P**OSITRON emission tomography (PET) systems operating in three-dimensional (3-D) mode do not collimate events

Manuscript received December 2, 1996; revised October 30, 1998. This work was supported by the Medical Research Council of Canada under Grants SP-30 and MT11541. The Associate Editor responsible for coordinating the review of this paper and recommending its publication was D. Townsend. *Asterisk indicates corresponding author.*

J. J. Moreno-Cantú is with the Department of Neurology and Neurosurgery, Montreal Neurological Institute, McGill University, Montreal, QC. H3A 2B4 Canada.

\*C. J. Thompson is with the McConnell Brain Imaging Centre, Montreal Neurological Institute, McGill University, Montreal, QC. H3A 2B4 Canada (e-mail: chris@bic.mni.mcgill.ca).

R. J. Zatorre is with the Department of Neuropsychology, Montreal Neurological Institute, McGill University, Montreal, QC. H3A 2B4 Canada.

Publisher Item Identifier S 0278-0062(98)09736-5.

that originate within their field-of-view (FOV). This makes 3-D PET scanners particularly sensitive to the detection of single and random events. Such events decrease scanner performance by generating detector dead time. Although the effect of dead time in 3-D scanners can be reduced by spreading the total per-subject dose over as many injections as possible so only a few mCi are used per scan [1], practical considerations limit the number of injections used per subject. This results in a trade-off amongst counting statistics, scanner efficiency and the practical constraints experienced when imaging subjects or neurological patients in a clinical facility. Some of these practical constraining factors are: 1) the length of the scanning session; 2) volunteer or patient tolerance; 3) the time allocated/project in a multiuser shared imaging facility; and 4) a finite number of stimuli (particularly for cognitive tasks where stimulus novelty plays a key role). After performing hundreds of  $H_2^{15}O$  bolus activation experiments on volunteers and neurological patients at our institution, we have observed that scanning sessions involving normal volunteers spanning longer than three hours are very difficult to perform (this view is also shared at other PET centers [2]). Similar sessions involving neurological patients are even more difficult to accomplish. In studies employing regional-cerebral-blood-flow (rCBF) [3], [4], standard activity-concentration [5], [6], switched [7], [8] and cold-bolus/switched (CBS) [9] protocols, the time limitation enables scanning sessions with an average of 12 injections/subject (each session includes time for positioning the subject, a transmission scan and 10–12 min between scans to allow for isotope decay). In studies employing background-subtraction protocols [10], the time interval between scans may be reduced enabling the acquisition of more scans/session.

In this paper, we discuss dose fractionation strategies, for the protocols mentioned above, that account for the scanner performance and the practical aspects of imaging volunteers and neurological patients in same-day one-session studies (i.e., image data from a subject cannot be collected over several sessions spread on several days—this is commonly the case in studies of neurological patients or of volunteers scanned in a multiuser imaging facility). These protocols were selected for study because: 1) rCBF protocols are the gold-standard when investigating brain function with  $H_2^{15}O$ ; 2) standard activity concentration protocols are commonly used to enhance the signal-to-noise ratio (SNR) of subtracted images; 3) switched

protocols have been proven to yield significant improvements to the SNR when compared to equivalent images obtained with standard activity concentration protocols and are as easy to implement as their standard counterpart; and 4) CBS protocols yield SNR enhancements even larger than those obtained with switched protocols although they are more difficult to implement.

### A. Description of $H_2^{15}O$ Bolus Acquisition Protocols

In activation studies, brain function is commonly investigated by comparing PET images acquired when subjects perform different tasks [11], [12]. When using a standard activation protocol (i.e., rCBF or activity-concentration protocols), data are acquired while subjects perform an activation or a baseline task throughout the scanning period. Standard-protocol scans acquired in order to provide quantitative measurements of rCBF are collected for 40–60 s after the tracer arrives in the brain [3], [4] while standard-protocol scans optimizing the SNR of subtracted images are typically 60-s to 100-s long [5], [6]. Longer standard-protocol scans are not used since the SNR of the resulting activation images becomes smaller [5], [6]. Switched and CBS protocols enhance the SNR of subtracted activation images by manipulating tracer kinetics in order to maintain the difference between activation and baseline signals longer than standard protocols. This allows the acquisition of scans up to 4-min long [7]. In these protocols, the subtracted signal is prolonged by reducing tracer washout from activated regions during the washout phase of the input function while increasing washout from nonactivated regions. This is accomplished by switching task execution at the time that tracer concentration in the brain reaches a maximum from activation to baseline in activation scans and vice versa in baseline scans. Activation studies employing switched protocols have reported increases of up to 38% in the statistical significance of activation foci observed across subjects when compared to equivalent measurements obtained using standard rCBF protocols [7], [8]. These increases have been shown to be a result of decreased image noise yielded by the longer acquisition times obtainable through task-switching [8]. CBS protocols enhance even further the SNR gains obtained with switched protocols by combining task switching with the release of a large activity-free bolus (cold bolus). The cold bolus is formed by occluding blood circulation to the lower limbs prior to tracer injection [9] using pressure cuffs placed on both legs at upper thigh level. The cuffs are inflated above arterial pressure a few seconds prior to bolus injection thereby isolating about 20%–40% of the total blood volume in the lower extremities. When activity concentration in the brain reaches a maximum, typically 40–60 s after isotope injection, the cuffs are released and the subject switches task execution. The effect of using a cold-bolus is two fold. First, lower-limb circulation occlusion decreases tracer dispersion during the uptake phase of the input function therefore increasing tracer uptake in the brain. Second, release of the cold-bolus increases tracer washout from baseline regions during the washout phase of the input function since it is combined with task-switching. In PET experiments comparing activation foci obtained with

TABLE I  
CTI ECTA EXACT HR+ : PHYSICAL CHARACTERISTICS

Gantry type:	whole body
Axial field-of-view (FOV):	15.5 cm
Scintillation material:	BGO
Number of crystal block rings:	4
"    blocks/ring:	72
"    crystals/block:	8x8
Number of crystal rings:	32
Crystal size (mm):	4.05(axial)x4.39(circumferential)x30(radial)
Number of crystals:	18432
Inter-plane septa:	removable
Imaging modes supported:	2D/3D/whole body
Transaxial resolution (mm)†:	5.1 FWHM ‡ at 1cm from FOV's centre
	6.6 " 10cm " "
Axial resolution (mm)†:	4.2 " 0.4cm " "
	5.4 " 9.0cm " "
<b>3D mode -count rates NEMA 20 cm-diameter phantom (1<math>\mu</math>Ci/ml)†</b>	
prompts	466 kps
randoms	1016 kps
dead time	73 %

† measured at our institution during scanner's acceptance tests; quantities shown correspond to total system rates.

‡ full-width-at-half-maximum

CBS and switched protocols, the CBS protocol yielded mean improvements of up to 36% to the statistical significance of the activation foci. CBS protocols [9] enhance the SNR of activation images by increasing tracer concentration during the uptake phase of the input function and by decreasing tracer concentration during the washout phase.

### B. Objectives of This Study

The work presented in this manuscript describes: 1) the performance of the ECAT<sup>1</sup> EXACT HR+ whole body positron emission tomograph [13], [14] when employed to study brain function using rCBF  $H_2^{15}O$  bolus activation protocols in 3-D mode; 2) dose fractionation strategies to be used routinely in same-day one-session  $H_2^{15}O$  bolus activation studies that account for the scanner count-rate performance and the practical aspects of acquiring data from volunteers and neurological patients with rCBF protocols; and 3) an analysis of possible dose fractionation strategies to be employed when measuring brain function with protocols that maximize the SNR of subtracted images by manipulating tracer kinetics such as the switched and CBS protocols. In addition, this work is discussed in the context of data acquisition techniques that employ background image subtraction to decrease the time between consecutive scans.

## II. METHODS

### A. PET Experiments

Five healthy right-handed volunteers ( four males and one female; mean age 24 yrs) were scanned using the ECAT EXACT HR+ in 3-D mode in order to measure regional changes of cerebral blood flow (Table I). All volunteers gave informed consent and were scanned in compliance with the medico-ethical guidelines in effect at the Montreal Neurological Institute and Hospital.

<sup>1</sup>Manufactured by CTI Inc., Knoxville TN.

1) *Scanning Conditions*: The scans used a fast ( $\sim 3$  s) intravenous bolus injection of  $H_2^{15}O$  as the radioactive tracer; a 14-s delay between injection and acquisition to allow for tracer arrival into the brain; and were 60-s long. The subjects lay on the scanner's bed with their eyes closed in a quiet darkened room.

2) *Activation and Baseline Scans*: The scans performed were either activation or baseline scans depending on the stimulus presented to the subjects during data acquisition. Two types of activation scans and one type of baseline scan were used. Vibrotactile and auditory stimulations were employed for the activation scans while a resting condition was used for the baseline scans.

3) *Activation Scans*: Subjects were asked to concentrate on the stimulus which started concurrently with bolus injection and was maintained until data acquisition ended.

- a) *Auditory stimulation*: White noise bursts of 75 dB (sound pressure level) of intensity; 500 ms long and 500 ms apart were played to the subjects binaurally through insert earphones (Eartone3A<sup>TM</sup>).
- b) *Vibrotactile stimulation*: Subjects had the moving head of a vibrator (Thrive<sup>TM</sup>) fixed to the fingers of their right hands, while their right arms were fully extended and placed on a cushion to isolate the vibration to the fingers only. The vibrator was pulsed on and off at a frequency of 1 Hz.

4) *Baseline Scans*: Subjects were asked to relax and rest. The earplugs and vibrator were kept in the positions used during the activation scans but no stimulus was presented.

5) *Data Acquisition*: The subjects were required to participate in each of the three scans described above with injected activities of 5, 10, 15, and 20 mCi for a total of 12 scans per subject (one subject underwent only ten scans because of cyclotron malfunction). The maximum activity used per injection was 20 mCi since in a 12-injection study this delivers the maximum accumulated dose that can be administered to volunteers according to regulations in effect at our institution. All scans were acquired in 3-D mode (no septa in the scanner FOV) using the scanner default settings and were reconstructed using in-plane and axial Hanning filters with 0.3 cycles per sample cut-off frequency (Table II). The order for scan-acquisition/task-execution was counterbalanced within and across subjects to reduce the effect of task adaptation since the imaged tasks were performed several times by each subject [15], [16]. The subjects also underwent magnetic resonance (MR) scans which were registered to their corresponding PET scans to facilitate the anatomical localization of activation foci [17].

6) *Data Analysis*: The scans were divided into eight separate and independent sets according to the type of stimulation employed and the activity of the injected tracer. Thus, separate vibrotactile- and auditory-stimulation sets were formed for

TABLE II  
DATA ACQUISITION AND RECONSTRUCTION PARAMETERS

	Acquisition	Reconstruction (image: 128x128 pixels)
Axial FOV	15.52	Corrections:
Interplane septa	retracted	scattered and random events
Energy thresholds	650/350 Kev	decay
Sinogram mode	prompts-delays	normalization
Span/Ring difference†	9/22	arc (spherical geometry)‡
Coincidence window	12 nsec	3D attenuation
Frames/Time/Delay	1/60 sec/14 sec	Filter:Hanning (cutoff=0.3cycles/sample)††

†Span=number of possible lines of response in odd and even planes as a result of plane interleaving; Ring difference=largest absolute difference in detector ring numbers accepted by the scanner.

‡Corrects for the scanner's spherical geometry.

††Hanning filter  $c(f)=0.5|f|(1+\cos(\pi f/f_m))$  if  $|f| \leq f_m$  and 0 otherwise where  $f_m=0.3$  cycles/sample. This cutoff frequency corresponds to a spatial resolution of 8 mm FWHM.

activities of 5, 10, 15, and 20 mCi. For each set, a SNR image was generated for the mean change in normalized activity between baseline and activation scans using a standard deviation pooled across all intracerebral voxels as an estimation of the image noise[18]. In brief, the SNR images for each of the eight sets were created as follows: a) individual scans are smoothed to overcome across-subjects anatomical variability [14-mm full-width-at-half-maximum (FWHM)], transformed into a stereotaxic coordinate system [17], [19], and normalized to have a mean of 100; b) baseline scans are subtracted from the activation scans and the resulting images are averaged across subjects into a magnitude image; c) a standard deviation image of the subtracted scans included in the average is generated; d) the standard deviation pooled across all intracerebral voxels in the standard deviation image is calculated; e) SNR values for voxels in the averaged image were computed by dividing each voxel value by the pooled standard deviation of the image. The anatomical location of activation foci was determined from the averaged-across-subjects co-registered MR volumes in Talaraich space [19].

## B. Scanner Evaluation Parameters

The evaluation of the scanner performance was based on observations of the correlation between injected activity and the following parameters and image characteristics: 1) dead time; 2) detected true events; 3) correction for random and scattered events; 4) image noise; and 5) magnitude and significance of activation foci associated with the tasks described above. In addition, estimations of the noise effective counts (NEC) were used as a figure-of-merit encompassing the main imaging variables.

NEC values were calculated as [20] (1), shown at the bottom of the page, where  $f$  is the fraction of lines of response in the sinogram passing through the subjects' heads (estimated to be 0.3) while the factor "2" accounts for the increased noise variance of the randoms component since random events are calculated using delayed coincidences. The NEC values shown here used an estimated scatter count fraction of 45%. The

$$NEC = \frac{(\text{true events})^2}{(\text{true events} + \text{scattered events} + (2f)\text{random events})} \quad (1)$$

scanner dead time was studied as a function of the injected dose and the time elapsed after bolus injection. Dead time data were obtained from on-line calculations provided by the scanner's acquisition software supplied by the manufacturer. The efficacy of the corrections for random and scattered events across the injected doses was roughly estimated by comparing voxel intensity measurements from activity free brain regions, such as the cerebral ventricles, to grey matter regions. The effect of the injected dose on the ability to detect foci of neuronal activation was evaluated by assessing the correlation between the significance of the signals from each of the expected activation foci and the activity injected. Likewise, the correlation amongst injected activity, image noise, SNR, and the data-acquisition protocol used was investigated in the acquired data.

### III. RESULTS AND DISCUSSION

#### A. Evaluation of Scanner Sensitivity, Efficiency, and Ability to Correct for Spurious Counts

Fig. 1 shows the behavior of the total uncorrected coincidences (prompts), the estimated total random events (delayed), and the total true events (trues + scatter)<sup>2</sup> averaged across all subjects and across stimulus conditions as a function of the injected dose. As shown in the figure, the scanner relative sensitivity to true events decreased as the dose increased while the number of detected random events increased with the dose. Thus, over 70% of all detected events were trues when injecting 5 mCi, while only 50% of the events were trues when the dose increased to 20 mCi. Fig. 2 shows the estimated noise effective counts also obtained by averaging individual scans across subjects and across tasks. These measurements suggest that the NEC values plateau after 10 mCi and that use of 15 or 20 mCi/injection does not yield NEC values significantly different than those obtained using 10 mCi/scan. This finding is similar to those previously described for the GE Advance system in 3-D mode [21]. Fig. 3 describes the observed scanner mean dead time measurements for the injected doses investigated. The plotted values were derived by averaging across subjects the observed dead times throughout the scan periods. Dead time grew linearly from just over 10% when 5 mCi injections were used to over 25% when 20 mCi were injected. The scanner's ability to correct for random and scattered events was roughly estimated by measuring voxel values in regions without tracer concentration, such as the lateral ventricles, and comparing them to values from grey matter regions in activated and baseline states. These measurements suggest that scattered and random events were corrected for all the injected activities tested since no significant differences were observed amongst the calculated ratios. A more accurate estimation of the effectiveness of the corrections is not needed since, in activation studies, random and scattered events mostly cancel out during subtraction of images of the same activity making these corrections unnecessary [22], [23].

<sup>2</sup>In Fig. 1 and throughout its description, the term true events refers to scattered and unscattered coincident events.

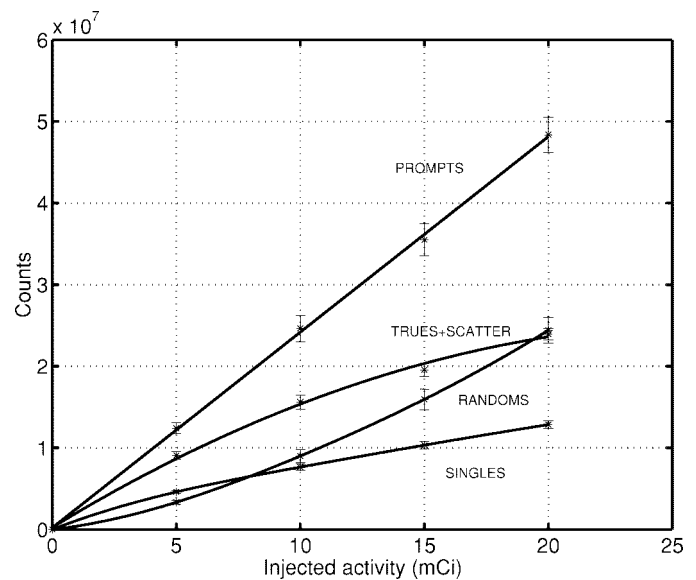


Fig. 1. Distribution of mean uncorrected coincidence (prompts), true (scattered and unscattered), random (delayed), and single events across the injected activities. Mean values were calculated by averaging measurements resulting from scans with the same injected activity across subjects. Error bars show the standard error of the means.

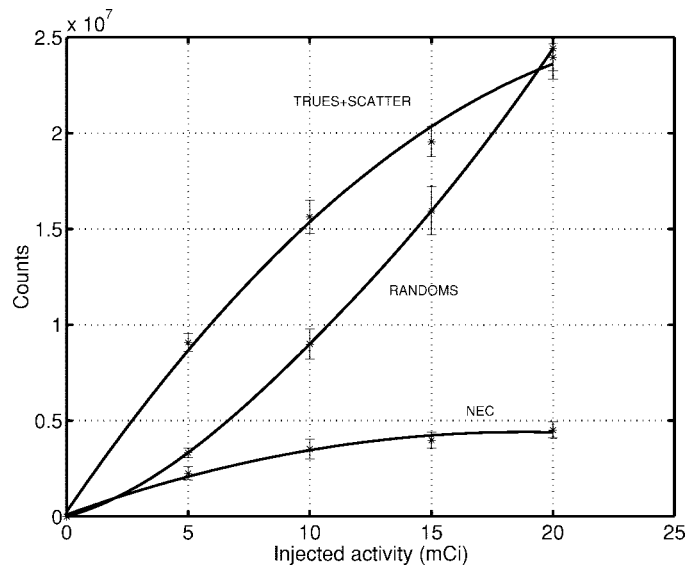


Fig. 2. Mean noise effective counts (NEC) as a function of injected activity for 3-D scans [see (1)].

#### B. Injected Dose and the Significance of the Expected Activation Foci

Fig. 4 shows the ratio of the mean subtracted signal from the detected foci and the overall image noise as estimated by the standard deviation pooled across all the intracerebral voxels. The activation foci were located in the left primary somatosensory cortex for scans where the vibrotactile stimulus was used [16] and in the bilateral primary auditory cortex for scans where the auditory stimulus was used [24], [25]. For an ideal scanner (i.e., one whose performance is constant independently of the activity used), the difference between activated and baseline signals is expected to remain constant across the injected activities since the images are

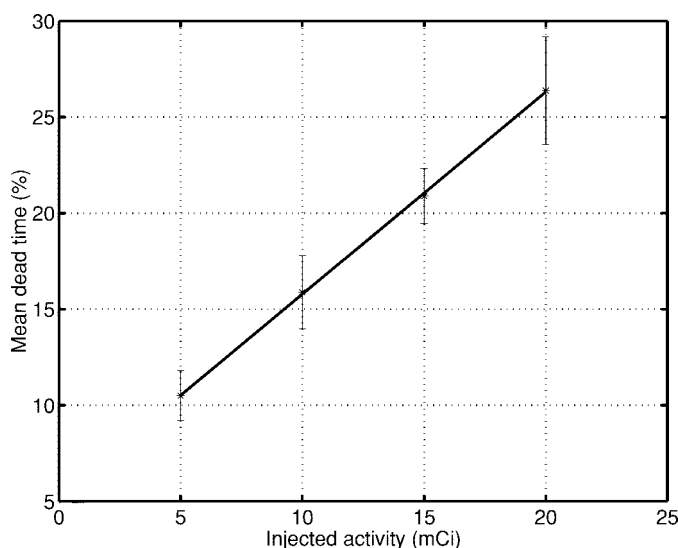


Fig. 3. Mean scan dead time across activities. The error bars (sample standard deviation) describe the observed variability of the dead time within each scan in each activity group.

normalized to have the same mean number of counts before subtraction. Thus, if any pattern of variability in the SNR across the injected activities were to be observed, this would be introduced by changes in the overall image noise. On the other hand, if image noise were only caused by the statistical variability associated with measurements of isotope concentration, the overall image noise would be expected to change proportionally with a  $(\text{counts})^{1/2}$  pattern. In the measurements performed here, variations of the normalized relative signal magnitude for a given stimulus are expected to be introduced mainly by head movements and changes in the rCBF response caused by task habituation and stimulus attention. As explained before, the effect of these factors on the relationship between signal magnitude and injected dose was expected to be minimized by counterbalancing the scan order across and within subjects. The large variability across same-activity measurements, depicted by the error bars in the figure, suggests that their effect was not totally eliminated, most likely because the sample size/activity level was small. Nevertheless, the data shown in Fig. 4 suggests that, for the activity levels tested, the SNR grew as the injected activity increased. The highest SNR measurements were observed when the 20 mCi injections were used.

Visual inspection of the images from different doses revealed no obvious changes in resolution or noise reduction across the injected doses. Images of the same structures across the injected doses were indistinguishable to the naked eye. As mentioned above, when brain function is investigated using normalized images, the relative magnitude of the signals from activation foci with respect to the signal from baseline regions is independent from the injected dose. However, image noise is correlated to the total amount of counts in individual scans and therefore is correlated to the injected activity. Figs. 5 and 6 describe the observed correlation between image noise and injected activity using variability measurements in regions-of-interest (ROI's) and across all the intracerebral voxels in the averaged subtracted scans respectively. Fig. 5 shows the

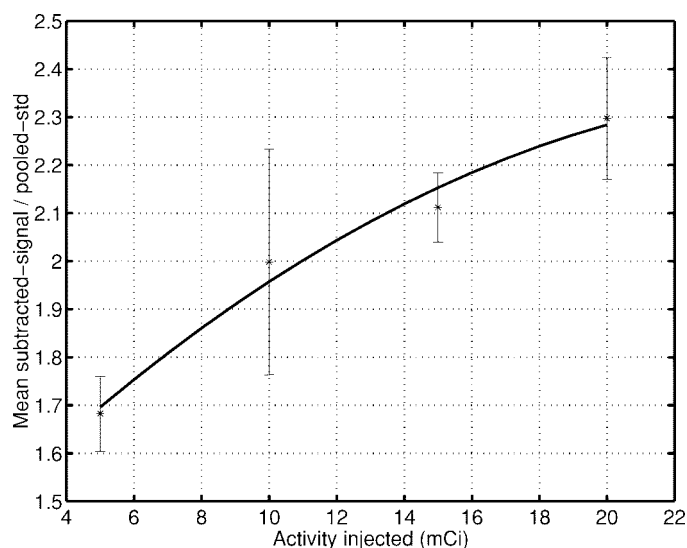


Fig. 4. Average significance of the signals from the detected activation foci relative to the image standard deviation. The foci were located in the left primary sensory and bilateral primary auditory cortices. Error bars show the standard error of the means.

effect of injected activity on noise measured by placing 3-mm radius ROI's over the left cerebellum, right cingulate and right frontal cortices in the averaged subtracted image for each of the activities tested. The figure shows the percent ratio between the values of the mean noise ROI and the values of mean signal ROI. As expected, variability decreased as the injected dose increased. The minimum variability was observed in the 20 mCi data set. The reductions in image noise caused by increasing the injected dose from 10 mCi to 15 or 20 mCi was marginal when compared to the reduction observed when increasing from 5 to 10 mCi. Similar findings were observed when the variability across all intracerebral voxels was used as measurement of image noise (Fig. 6). The noise/dose correlation shown in Figs. 5 and 6 was calculated in data sets reconstructed at a resolution of 14 mm FWHM. Activation studies employing across-subject image averaging are commonly smoothed to a lower resolution (18- to 20-mm FWHM) to compensate for intersubject anatomical variability. If lower resolution images are used, the noise-level differences amongst the tested doses will become smaller. In that case, the noise reductions observed when injecting doses greater than 10 mCi will be even weaker.

In the case of activation studies employing protocols designed to maximize the SNR of subtracted images, such as the switched [7], [8] and the CBS [9] protocols, the effect of the injected dose in the 5–20 mCi range is likely to have a larger impact on image noise and therefore on the significance of the activation foci. This occurs because these protocols use significantly longer scanning times than standard rCBF activation protocols like the one used here. Switched and CBS protocols enhance the SNR by manipulating tracer uptake and washout in order to prolong the difference in the signal from neuronal substrates with high (activation) and low (baseline) blood flow. As described before, an activation study using one of these protocols employs scans up to 4-min long, while a similar study employing a standard protocol uses scans 40- to

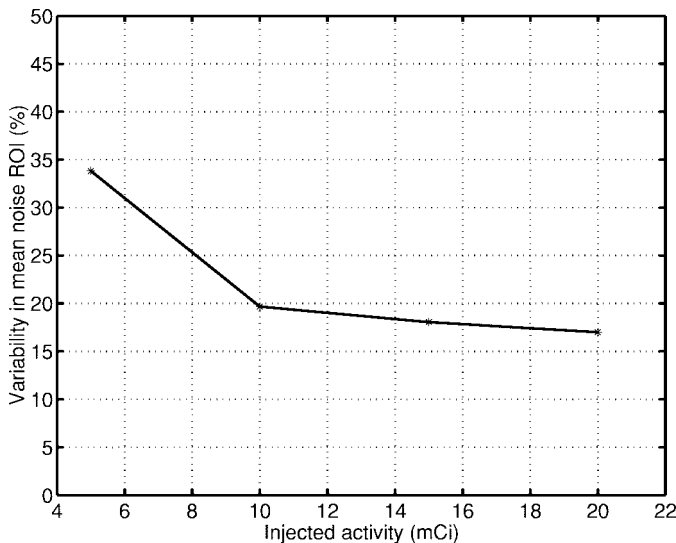


Fig. 5. Mean noise-to-signal ratio. Values shown were calculated from noise ROI's in right superior frontal, cingulate and left cerebellar regions; and from signal ROI's over the three activation foci detected.

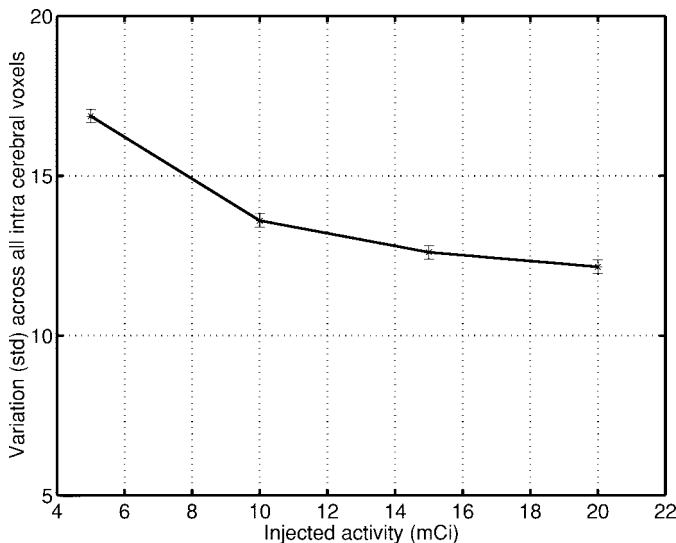


Fig. 6. Variability across all intracerebral voxels (averaged across subjects). Error bars show the standard error of the means.

60-s long if measuring rCBF changes or scans 60–100 s long if measuring differences of isotope-concentration. As shown in Figs. 5 and 6, increasing the injected dose from 10 mCi to 15 or 20 mCi only marginally reduced the image noise, however, larger reductions were observed between 5 and 10 mCi. Since in 4-min scans the tracer will have decayed two half-lives during data acquisition, an initial injection of 20 mCi will provide 10 mCi at the start of the second half of a scan compared to only 5 mCi if a 10 mCi injection is used. The data collected at these radioactivity levels are likely to exhibit significant noise differences as suggested by the measurements shown in Figs. 5 and 6. The relative contribution of the signal (and its statistical variability) from different periods in a scan on the overall focus SNR was evaluated using a standard one-compartment model [26], [9] of tracer kinetics and a typical measured input function produced by a  $\text{H}_2^{15}\text{O}$  bolus injection

[27]. The model estimates the uptake of  $\text{H}_2^{15}\text{O}$  in tissue under baseline (low flow) and activation (high flow) conditions throughout the different stages of the input function. Since our data were only collected in 1-min scans, this model was used to investigate the effect that variations on the counts collected 2–4 min after injection have on the accumulated signal and its estimated statistical variability for switched and CBS protocols. Reductions of 10%, 20%, and 30% to the signal variability in the counts collected between 2 and 4 min were studied. The reductions yielded 4%, 7%, and 10% increases in the overall SNR when a switched protocol was employed and 3%, 5%, and 7% increases when a CBS protocol was used. The relative increases observed in CBS protocol are slightly smaller than those obtained with a switched protocol since the integrated subtracted signal in the former protocol is larger [9]. In activation studies employing background subtraction in order to decrease the time interval between consecutive scans, the use of 15 or 20 mCi injections is not expected to yield significant gains in noise reduction if the data are collected in short scans (unless this method were to be combined with a switched or CBS acquisition scheme).

It is also important to note that these studies were done with delayed counts subtracted from the sinogram containing prompt counts (trues + scattered + random events). It has been suggested that the noise due to random events can be reduced by acquiring delayed counts in a separate sinogram and then subtract a smoothed version of the delayed counts from the prompt counts [20]. This would potentially decrease the noise present in high activity studies were random counts are the highest source of noise. However, use of this technique doubles the amount of data storage requirements during data acquisition and archiving. Furthermore, the noise in PET activation images generated employing averaging of subtracted data sets could also be decreased by eliminating correction for random events [22], [28]. Since the distribution and magnitude of the random events is likely to remain approximately constant in intra subject images of the same injected activity, subtracting such images would eliminate the random event component from the subtracted image.

#### IV. CONCLUSIONS

In this paper, the following issues were described: 1) the performance characteristics of the Siemens ECAT EXACT HR+ 3-D whole body PET scanner when used to investigate brain function with rCBF  $\text{H}_2^{15}\text{O}$  bolus activation protocols; 2) the effect of dose fractionation strategies in the magnitude and significance level of activation signals measured using a one-session 12-injection rCBF activation protocol designed to account for the scanner performance as well as the practical aspects of studying neurological patients and normal volunteers in a multiuser PET imaging facility; and 3) possible dose fractionation strategies to be employed when measuring brain function with protocols that maximize the SNR of subtracted images by manipulating tracer kinetics in order to extend scan length such as the switched and CBS protocols.

### A. The ECAT EXACT HR+ Across the 5- to 20-mCi Range

1) *Performance Characteristics*: a) dead time grew linearly from 10% to 25%; b) random events increased from 30% to 50% of the detected events; c) scattered and random events appear to be adequately removed by the scanner's software; and d) NEC values reached a plateau after 10 mCi.

2) *One-Session 12-Injection H<sub>2</sub><sup>15</sup>O Bolus PET Activation Protocols*: a) When measuring brain function with a standard rCBF protocol, bolus injections of 20 mCi yielded activation foci with the highest SNR, however, the noise reductions obtained by injecting more than 10 mCi are small; and b) the SNR in protocols employing long scanning periods, such as the switched and CBS protocols, is likely to be maximized if 20-mCi injections are used.

### ACKNOWLEDGMENT

The authors would like to thank Dr. E. Meyer, Dr. D. Reutens, and P. Neelin for their suggestions. They would also like to thank R. Fukasawa, G. Sauchuk, and A. Casavant for their diligent cooperation during the scanning sessions. Finally, they would like to thank the medical cyclotron personnel for the preparation of the radioisotopes.

### REFERENCES

- [1] S. R. Cherry, R. P. Woods, E. J. Hoffman, and J. C. Mazziotta, "Improved detection of focal cerebral blood flow changes using three-dimensional positron emission tomography," *J. Cereb. Blood Flow Metab.*, vol. 13, no. 4, pp. 630–8, 1993.
- [2] R. S. Frackowiak and K. J. Friston, "Functional neuroanatomy of the human brain: Positron emission tomography—A new neuroanatomical technique," *J. Anat.*, vol. 184, pp. 211–225, 1994.
- [3] P. Herscovitch, J. Markham, and M. E. Raichle, "Brain blood flow measured with intravenous H<sub>2</sub><sup>15</sup>O. (I) Theory and error analysis," *J. Nucl. Med.*, vol. 24, pp. 782–789, 1983.
- [4] M. E. Raichle, W. R. W. Martin, P. Herscovitch, M. A. Mintun, J. Markham, "Brain blood flow measured with intravenous H<sub>2</sub><sup>15</sup>O. II. Implementation and validation," *J. Nucl. Med.*, vol. 24, pp. 790–798, 1983.
- [5] I. Kanno, H. Iida, S. Miura, and M. Murakami, "Optimal scan time of oxygen-15-labeled water injection method for measurements of cerebral blood flow," *J. Nucl. Med.*, vol. 32, pp. 1931–1934, 1991.
- [6] M. A. Mintun, M. E. Raichle, and R. P. Quarles, "Length of PET data acquisition inversely affects ability to detect focal areas of brain activation," *J. Cereb. Blood Flow Metab.*, vol. 9, Suppl-1:S349, 1989.
- [7] S. R. Cherry, R. P. Woods, N. K. Doshi, P. K. Banerjee, and J. C. Mazziotta, "Improved signal-to-noise in PET activation studies using switched paradigms," *J. Nucl. Med.*, vol. 36, pp. 307–314, 1995.
- [8] J. J. Moreno-Cantú, D. C. Reutens, C. J. Thompson, R. J. Zatorre, D. Klein, E. Meyer, and M. Petrides, "Signal-enhancing switched protocols to study higher-order cognitive tasks with PET," *J. Nucl. Med.*, vol. 39, pp. 350–356, 1998.
- [9] J. J. Moreno-Cantú, C. J. Thompson, E. Meyer, P. Fiset, R. J. Zatorre, D. Klein, and D. Reutens, "Enhancement of the signal-to-noise ratio in H<sub>2</sub><sup>15</sup>O bolus PET activation studies using a combined cold-bolus/switched protocol," in *Quantitative Functional Brain Imaging with Positron Emission Tomography*, R. E. Carson, M. E. Daube-Witherspoon, and P. Herscovitch, Eds. Bethesda, MD: Academic, June 1997.
- [10] G. F. Eden, K. Keil, J. M. Maisog, R. E. Carson, P. Herscovitch, and J. V. Haxby, "PET H<sub>2</sub><sup>15</sup>O activation studies using a short interscan interval and background-subtraction technique," *Neuroimage*, vol. 3, no. 3, p. S19, 1996.
- [11] P. T. Fox, M. A. Mintun, E. M. Reiman, and M. E. Raichle, "Enhanced detection of focal brain responses using interscan averaging and change-distribution analysis of subtracted PET images," *J. Cereb. Blood Flow Metab.*, vol. 8, pp. 642–653, 1988.
- [12] J. C. Mazziotta and M. E. Phelps, "Positron emission tomography studies of the brain," in *Positron Emission Tomography and Autoradiography. Principles and Applications for the Brain and Heart*, M. E. Phelps, J. C. Mazziotta, and H. R. Schelbert, Eds. New York: Raven, 1986, pp. 493–579.
- [13] L.-E. Adam, J. Zaers, H. Ostertag, H. Trojan, M. E. Bellemann, and G. Brix, "Performance evaluation of the whole-body PET scanner ECAT EXACT HR+ following the IEC standard," *IEEE Trans. Nucl. Sci.*, vol. 44, pp. 1172–1179, 1997.
- [14] J. Z. Bellemann, L. E. Adam, H. Ostertag, G. Brix, H. Trojan, and J. Doll, "Performance characteristics of the PET scanner ECAT EXACT HR+ following the NEMA protocol," presented at *ECAT Tech. Users Meet.*, Stockholm Sweden, 1996, A-10.
- [15] M. E. Raichle, V. A. Fiez, and T. O. Videen *et al.*, "Practice-related changes in human brain functional anatomy during nonmotor learning," *Cereb. Cortex*, vol. 4, no. 1, pp. 8–26, 1994.
- [16] E. Meyer, S. S. Ferguson, and R. J. Zatorre *et al.*, "Attention modulates somatosensory cerebral blood flow response to vibrotactile stimulation as measured by positron emission tomography," *Ann. Neurol.*, vol. 29, no. 4, pp. 440–443, 1991.
- [17] A. C. Evans, S. Marret, P. Neelin, L. Collins, K. Worsley, W. Dai, S. Milot, E. Meyer, and D. Bub, "Anatomical mapping of functional activation in stereotactic coordinate space," *Neuroimage*, vol. 1, pp. 43–53, 1992.
- [18] K. J. Worsley, A. C. Evans, S. Marrett, and P. Neelin, "A three-dimensional statistical analysis for CBF activation studies in human brain," *J. Cereb. Blood Flow Metab.*, vol. 12, pp. 900–918, 1992.
- [19] J. Talairach and P. Tournoux, "Co-planar stereotaxic atlas of the human brain." New York: Thieme Medical, 1988.
- [20] S. C. Strother, M. E. Casey, and E. J. Hoffman, "Measuring PET scanner sensitivity: Relating count rates to image signal-to-noise ratios using noise equivalent counts," *IEEE Trans Nucl. Sci.*, vol. 37, no. 2, pp. 783–788, 1990.
- [21] S. Holm, I. Law, O. B. Paulson, "3D PET activation studies with an H<sub>2</sub><sup>15</sup>O bolus injection: Count rate performance and dose optimization," R. Myers, V. Cunningham, D. Bailey, T. Jones, ed., in *Quantification of Brain Function Using PET*. San Diego, CA: Academic, 1996, pp. 93–97.
- [22] J. R. Votaw, "Signal-to-noise ratio in neuro activation PET studies," *IEEE Trans Med Imag.*, vol. 15, no. 2, pp. 197–205, 1996.
- [23] E. Paulesu, V. Bettinardi, M. Signorini, G. Striano, D. Perani, M. C. Gilardi, and F. Fazio, "Scatter correction and 3D PET activation rCBF studies," *Neuroimage*, vol. 3, no. 3, p. S36, 1996.
- [24] R. J. Zatorre, A. C. Evans, E. Meyer, and A. Gjedde, "Lateralization of phonetic and pitch discrimination in speech processing," *Sci.*, vol. 256, no. 5058, pp. 846–9, 1992.
- [25] V. B. Penhune, R. J. Zatorre, J. D. MacDonald, and A. C. Evans, "Interhemispheric anatomical differences in human primary auditory cortex: Probabilistic mapping and volume measurement from magnetic resonance scans," *Cereb. Cortex*, vol. 6, pp. 661–672, 1996.
- [26] S. S. Kety, "The theory and application of the exchange of inert gas at the lungs and tissues," *Pharmacol. Rev.*, vol. 3, pp. 1–41, 1951.
- [27] M. Vafaee, K. Murase, A. Gjedde, and E. Meyer, "Dispersion correction for automatic sampling of O-15-labeled H<sub>2</sub><sup>15</sup>O and red blood cells," in *Quantification of Brain Function Using PET*, R. Myers, V. Cunningham, D. Bailey, and T. Jones, Eds.. San Diego, CA: Academic, 1996, pp. 72–75.
- [28] J. J. Moreno-Cantú, Y. Ma, C. J. Thompson, R. J. Zatorre, and M. Petrides, "Re-evaluating the precision of localizing activation foci by identifying local maxima in subtracted PET images," Personal Communications.